

Flat and bent branes with inner structure in two-field mimetic gravity

Qian Xiang ^{1*}, Yi Zhong ^{2†}, Qun-Ying Xie ^{1,3‡}, and Li Zhao ^{1§}

¹ *Institute of Theoretical Physics,*

Lanzhou University, Lanzhou 730000, China

² *School of Physics and Electronics Science,*

Hunan University, Changsha 410082, China

³ *School of Information Science and Engineering,*

Lanzhou University, Lanzhou 730000, China

Abstract

Inspired by the work [Eur. Phys. J. C 78 (2018) 45], we study the linear tensor perturbation of both the flat and bent thick branes with inner structure in two-field mimetic gravity. The master equations for the linear tensor perturbations are derived by taking the transverse and traceless gauge. For the Minsowskii and Anti-de-Sitter brane, the brane systems are stable against the tensor perturbation. The effective potentials of the tensor perturbations of both the flat and bent thick branes are volcano-like, and this structure may potentially lead to the zero-mode and the resonant modes of the tensor perturbation. We further illustrate the results of massive resonant modes.

* Email:xiangq18@lzu.edu.cn

† Email:zhongy@hnu.edu.cn

‡ Email:xieqy@lzu.edu.cn

§ Email:lizhao@lzu.edu.cn, corresponding author

I. INTRODUCTION

The braneworld theory has received much attention over the past years since it proposes a new route to possibly solve the gauge hierarchy problem and the cosmological constant problem [1–4]. The Randall-Sundrum (RS) models [3, 4] are the typical examples of them with a non-factorizable metric and a warped extra dimension. It is shown that RS models give rise to thin brane profiles because the warp factor has cusp singularities at the brane positions. Several proposals for generalizing thin branes into thick branes have been presented in the literature. The thick branes are obtained by introducing one or more bulk scalar fields coupled to gravity [5–15], or realized by pure geometric frameworks without background matter fields considered in [16–19]. Most of the models study Minkowski branes, and a few of them consider the curvature of the embedded brane, which includes de Sitter (dS) or anti-de Sitter (AdS) geometry.

On the other hand, mimetic gravity is proposed by Chamseddine and Mukhanov [20] as one of the extensions of general relativity (GR). In the original setup, a physical metric $g_{\mu\nu}$ is defined in terms of an auxiliary metric $\tilde{g}_{\mu\nu}$ and a scalar field ϕ with the relation $g_{\mu\nu} = -\tilde{g}_{\mu\nu}g^{\alpha\beta}\partial_\alpha\phi\partial_\beta\phi$. This model regards the scalar field as the conformal degree of freedom to mimic cold dark matter. The mimetic model is then investigated by adding a potential $V(\phi)$ of the scalar field to explain the cosmological issues [21, 22]. With the appropriate choice of the potential, it is possible to provide an inflationary mechanism and a bouncing universe within this framework [21]. Therefore, this stimulates some interests in phenomenology and its observational viability [23–30], and leads to the Hamiltonian analyses of different mimetic models [31–35]. Mimetic gravity in various modified gravity theories has also been widely discussed in [36–46]. Another interest in mimetic gravity is to investigate the mimetic gravity in braneworld scenarios. The late-time cosmic expansion and inflation are investigated in the mimetic RS braneworld [24]. Following this work, the late time acceleration and perturbation behavior are studied for the brane-anti-brane system [47]. Later, the tensor and scalar perturbations on several thick branes are investigated in mimetic gravity [48].

As we know, the scalar fields are usually introduced to generate the topological defects such as kinks and domain walls for realizing the thick branes, so it is natural to generate the domain walls by the mimetic scalar fields. However, suffering from the ghost and gradient instabilities, the original mimetic theory with single field could not suffice [49]. For the single field mimetic scenario, one can go to a ghost-free theory by adding higher derivative terms to the original theory [50]. For the two-field extension of the mimetic gravity put forward in [51], the double scalar fields

version not only avoids the above problem but also allows us to construct the thick branes with a complicated inner structure. It is common to find the background solution of the thick branes via the first-order formalism [11] or the extension method [52]. However, in the two-field mimetic theory, the gravity and two mimetic scalars are coupled. It is relatively harder to find the domain wall solutions if the four-dimensional geometry is either flat or curved. In this work, we apply the reconstruction technique [53] to seek the background solutions of three cases of thick branes. The approach gives the form of the warp factor and scalar fields, and provides a direct way to investigate the other variables. We consider that the thick domain walls possess four-dimensional dS and AdS symmetries as well as the Poincaré one. Because dS and AdS branes have different inner structures from flat brane, it is of interest to consider the tensor perturbation of gravity on the bent branes.

The paper is organized as follows. In section II, we introduce the mimetic thick brane model and consider three cases of thick branes. In section III, we analyze the stability of the model under the linear tensor perturbation and study the localization of gravity zero-mode. Finally, a brief conclusion is presented in Section V. Throughout this paper, capital Latin letters M, N, \dots represent the five-dimensional coordinate indices running over 0, 1, 2, 3, 5, and lower-case Greek letters μ, ν, \dots represent the four-dimensional coordinate indices running over 0, 1, 2, 3.

II. BRANE SETUP AND FIELD EQUATIONS

We consider the five-dimensional two-field mimetic gravity where the action is the Einstein-Hilbert action constructed in terms of the physical metric g_{MN} . For our model, in the natural unit, the action can be written as a Lagrange multiplier formulation,

$$S = \int d^4x dy \sqrt{-g} \left(\frac{R}{2} + \mathcal{L}_m \right), \quad (1)$$

where the Lagrangian of the two interacting mimetic scalar field is generalized as,

$$\mathcal{L}_m = \lambda \left[g^{MN} \partial_M \phi_1 \partial_N \phi_1 + g^{MN} \partial_M \phi_2 \partial_N \phi_2 - U(\phi_1, \phi_2) \right] - V(\phi_1, \phi_2). \quad (2)$$

In the original mimetic model $U(\phi) = -1$, and here the potential is extended into the form of $U(\phi_1, \phi_2)$ with double mimetic fields. The Lagrange multiplier λ enforces the mimetic constraint,

$$g^{MN} \partial_M \phi_1 \partial_N \phi_1 + g^{MN} \partial_M \phi_2 \partial_N \phi_2 - U(\phi_1, \phi_2) = 0. \quad (3)$$

The variation of the action (1) concerning the metric g_{MN} and the two scalar fields (ϕ_1 and ϕ_2) yields the following field equations, respectively:

$$\begin{aligned}
G_{MN} + 2\lambda\partial_M\phi_1\partial_N\phi_1 + 2\lambda\partial_M\phi_2\partial_N\phi_2 - \mathcal{L}_m g_{MN} &= 0, \\
2\lambda\Box^{(5)}\phi_1 + 2\nabla_M\lambda\nabla^M\phi_1 + \lambda\frac{\partial U(\phi_1, \phi_2)}{\partial\phi_1} + \frac{\partial V(\phi_1, \phi_2)}{\partial\phi_1} &= 0, \\
2\lambda\Box^{(5)}\phi_2 + 2\nabla_M\lambda\nabla^M\phi_2 + \lambda\frac{\partial U(\phi_1, \phi_2)}{\partial\phi_2} + \frac{\partial V(\phi_1, \phi_2)}{\partial\phi_2} &= 0.
\end{aligned} \tag{4}$$

The line-element for a warped five-dimensional geometry is generally assumed as,

$$ds^2 = a^2(y)\hat{g}_{\mu\nu}dx^\mu dx^\nu + dy^2 \tag{5}$$

with y the extra spatial coordinate. We deal with $a = a(y)$, $\phi_1 = \phi_1(y)$ and $\phi_2 = \phi_2(y)$ when considering the static brane. The metrics $\hat{g}_{\mu\nu}$ on the branes reads,

$$\hat{g}_{\mu\nu} = \begin{cases} -dt^2 + (dx_1^2 + dx_2^2 + dx_3^2) & M_4 \text{ brane,} \\ -dt^2 + e^{2\sqrt{\Lambda_4}t}(dx_1^2 + dx_2^2 + dx_3^2) & \text{dS}_4 \text{ brane,} \\ e^{-2\sqrt{-\Lambda_4}x_3}(-dt^2 + dx_1^2 + dx_2^2) + dx_3^2 & \text{AdS}_4 \text{ brane,} \end{cases} \tag{6}$$

where Λ_4 is related to the four-dimensional cosmological constant of dS_4 or AdS_4 brane [54, 55].

We know that Eqs.(3) and (4) determine the solution of the brane system. There are three independent equations and six variables in this system. To solve this system, we should preset three variables. Based on the reconstruction technique, we will give the form of $a(y)$, $\phi_1(y)$, $\phi_2(y)$ and try to find the solution of $U(\phi_1, \phi_2)$, $V(\phi_1, \phi_2)$ and $\lambda(\phi_1, \phi_2)$. Here the warp factor $a(y)$ and the scalar fields $\phi_1(y)$, $\phi_2(y)$ are given by

$$a(y) = \text{sech}(k(y - b)) + \text{sech}(ky) + \text{sech}(k(y + b)), \tag{7}$$

$$\phi_1(y) = \tanh(k(y - b)) + \tanh(k(y + b)), \tag{8}$$

$$\phi_2(y) = \tanh(k(y - b)) - \tanh(k(y + b)), \tag{9}$$

where k and b are parameters with dimension mass and length, respectively. To display the configuration of $a(y)$, $\phi_1(y)$ and $\phi_2(y)$, we introduce the dimensionless quantities $\tilde{y} = ky$ and $\tilde{b} = kb$. The shapes of the warp factor and the two scalar fields are depicted in Fig. 1. The above warp factor indicates that the bulk space-time is asymptotically AdS, which is essential for the localization of gravitation. The brane splits from a single brane into three sub-branes as the parameter \tilde{b} increases. Thus, these branes have a rich inner structure. The scalar field $\phi_1(\tilde{y})$ supports the topological solution which changes from a single-kink to a double-kink configuration with the increasing of \tilde{b} .

Without loss of generality, the other scalar field $\phi_2(\tilde{y})$ is assumed as a non-topologically lump-like solution.

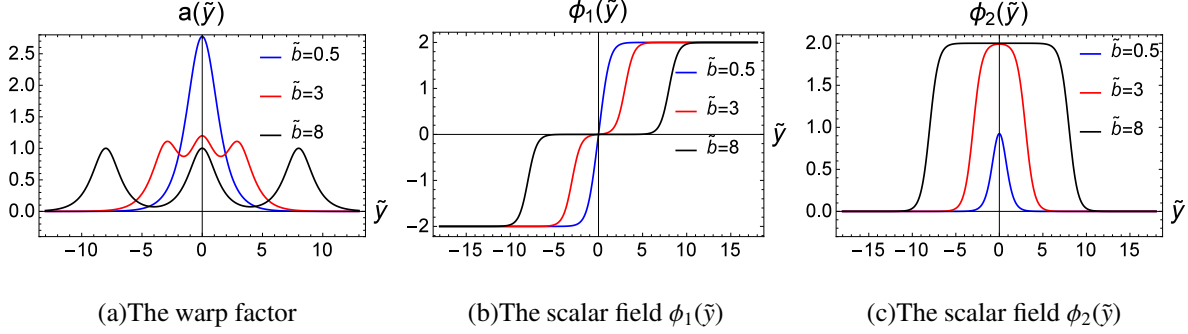


FIG. 1: Plots of the warp factor $a(\tilde{y})$ and two mimetic scalar fields $\phi_1(\tilde{y})$ and $\phi_2(\tilde{y})$ of the brane models.

A. Flat brane

For Minkowski brane, we take $\Lambda_4 = 0$. With the ansatz (6), the Einstein tensors are expressed as

$$G_{\mu\nu} = 3\eta_{\mu\nu} (a(y)a''(y) + a'(y)^2), \quad G_{55} = 6a'(y)^2/a(y)^2 \quad (10)$$

Eqs. (4) and (3) can be reduced to

$$\frac{3a'^2}{a^2} + \frac{3a''}{a} + V(\phi_1, \phi_2) + \lambda(U(\phi_1, \phi_2) - \phi_1'^2 - \phi_2'^2) = 0, \quad (11)$$

$$\frac{6a'^2}{a^2} + V(\phi_1, \phi_2) + \lambda(U(\phi_1, \phi_2) + \phi_1'^2 + \phi_2'^2) = 0, \quad (12)$$

$$\frac{8\lambda a' \phi_1'}{a} + 2\lambda \phi_1'' + 2\lambda' \phi_1' + \lambda \frac{\partial U(\phi_1, \phi_2)}{\partial \phi_1} + \frac{\partial V(\phi_1, \phi_2)}{\partial \phi_1} = 0, \quad (13)$$

$$\frac{8\lambda a' \phi_2'}{a} + 2\lambda \phi_2'' + 2\lambda' \phi_2' + \lambda \frac{\partial U(\phi_1, \phi_2)}{\partial \phi_2} + \frac{\partial V(\phi_1, \phi_2)}{\partial \phi_2} = 0, \quad (14)$$

$$\phi_1'^2 + \phi_2'^2 = U(\phi_1, \phi_2), \quad (15)$$

where the prime denotes the derivative with respect to y . Plugging Eqs. (7), (8) and (9) into (15), we get the following analytic solution,

$$\begin{aligned}
U(\phi_1(y), \phi_2(y)) &= 2k^2 \left[\text{sech}^4(k(y-b)) + \text{sech}^4(k(y+b)) \right], \\
V(\phi_1(y), \phi_2(y)) &= \frac{3k^2}{\left[\text{sech}(k(y-b)) + \text{sech}(k(y+b)) + \text{sech}(ky) \right]^2} \left[(\text{sech}(k(y-b)) \right. \\
&\quad + \text{sech}(k(y+b)) + \text{sech}(ky)) (\text{sech}^3(k(y-b)) - \frac{1}{2} (\cosh(2k(y+b)) - 3) \\
&\quad \times \text{sech}^3(k(y+b)) - \tanh^2(k(y-b)) \text{sech}(k(y-b)) + \text{sech}^3(ky) - \tanh^2(ky) \\
&\quad \times \text{sech}(ky)) - (\tanh(k(y-b)) \text{sech}(k(y-b)) + \tanh(k(y+b)) \text{sech}(k(y+b)) \\
&\quad \left. + \tanh(ky) \text{sech}(ky))^2 \right], \\
\lambda(\phi_1(y), \phi_2(y)) &= \frac{-3}{8 \left[\text{sech}(k(y-b)) + \text{sech}(k(y+b)) + \text{sech}(ky) \right]^2 \left[\text{sech}^4(k(y-b)) + \text{sech}^4(k(y+b)) \right]} \\
&\quad \times \left[2\text{sech}^4(k(y-b)) + 2\text{sech}^4(k(y+b)) + 2\text{sech}(ky) \text{sech}^3(k(y-b)) \right. \\
&\quad + (\cosh(2k(y-b)) + \cosh(2k(y+b)) - \cosh(4bk) + 3) \text{sech}^3(k(y-b)) \\
&\quad \times \text{sech}^3(k(y+b)) + \text{sech}^3(ky) (2\text{sech}(k(y-b)) + (\cosh(2k(y+b)) - \cosh(2bk) \\
&\quad \left. + \cosh(2ky) + 3) \text{sech}^3(k(y+b)) - 2 \sinh^2(bk) \text{sech}^3(k(y-b))) + 2\text{sech}^4(ky) \right]. \quad (16)
\end{aligned}$$

B. Bent branes

We now turn attention to the case of $\Lambda_4 \neq 0$. The presence of Λ_4 makes the field equation and background solution complex. For the dS_4 geometry ($\Lambda_4 > 0$), with the ansatz (6), the Einstein tensors are expressed as

$$\begin{aligned}
G_{\mu\nu} &= -\frac{3(\Lambda_4 - (a'(y))^2 - a(y)a''(y))}{a^2(y)} a^2(y) \hat{g}_{\mu\nu}, \\
G_{55} &= \frac{-6(\Lambda_4 - a'(y)^2)}{a^2(y)}. \quad (17)
\end{aligned}$$

Eqs. (4) and (3) can be reduced to

$$-\frac{3(\Lambda_4 - (a'(y))^2 - a(y)a''(y))}{a^2(y)} + V(\phi_1, \phi_2) + \lambda(U(\phi_1, \phi_2) - \phi_1'^2 - \phi_2'^2) = 0, \quad (18)$$

$$\frac{-6(\Lambda_4 - a'(y)^2)}{a^2(y)} + V(\phi_1, \phi_2) + \lambda(U(\phi_1, \phi_2) + \phi_1'^2 + \phi_2'^2) = 0, \quad (19)$$

$$\frac{8\lambda a'(y)\phi_1'}{a(y)} + 2\lambda\phi_1'' + 2\lambda'\phi_1' + \lambda\frac{\partial U(\phi_1, \phi_2)}{\partial\phi_1} + \frac{\partial V(\phi_1, \phi_2)}{\partial\phi_1} = 0, \quad (20)$$

$$\frac{8\lambda a'(y)\phi_2'}{a(y)} + 2\lambda\phi_2'' + 2\lambda'\phi_2' + \lambda\frac{\partial U(\phi_1, \phi_2)}{\partial\phi_2} + \frac{\partial V(\phi_1, \phi_2)}{\partial\phi_2} = 0, \quad (21)$$

$$\phi_1'^2 + \phi_2'^2 = U(\phi_1, \phi_2). \quad (22)$$

Now the system can be solved as,

$$\begin{aligned} U(\phi_1(y), \phi_2(y)) &= 2k^2 \left[\text{sech}^4(k(y-b)) + \text{sech}^4(k(y+b)) \right], \\ V(\phi_1(y), \phi_2(y)) &= \frac{3}{\left[\text{sech}(k(y-b)) + \text{sech}(k(y+b)) + \text{sech}(ky) \right]^2} \left[\Lambda_4 - k^2(\tanh(k(y-b)) \right. \\ &\quad \times \text{sech}(k(y-b)) + \tanh(k(y+b))\text{sech}(k(y+b)) + \tanh(ky)\text{sech}(ky))^2 \\ &\quad + k^2(\text{sech}(k(y-b)) + \text{sech}(k(y+b)) + \text{sech}(ky)) \\ &\quad \times (\text{sech}^3(k(y-b)) - \frac{1}{2}(\cosh(2k(y+b)) - 3)\text{sech}^3(k(y+b)) \\ &\quad \left. - \tanh^2(k(y-b))\text{sech}(k(y-b)) + \text{sech}^3(ky) - \tanh^2(ky)\text{sech}(ky)) \right], \\ \lambda(\phi_1(y), \phi_2(y)) &= \frac{-3}{8k^2 \left[\text{sech}(k(y-b)) + \text{sech}(k(y+b)) + \text{sech}(ky) \right]^2 \left[\text{sech}^4(k(y-b)) + \text{sech}^4(k(y+b)) \right]} \\ &\quad \times \left[-2\Lambda_4 + 2k^2\text{sech}^4(k(y-b)) + 2k^2\text{sech}^4(k(y+b)) + 2k^2\text{sech}(ky)\text{sech}^3(k(y-b)) \right. \\ &\quad + k^2(\cosh(2k(y-b)) + \cosh(2k(y+b)) - \cosh(4bk) + 3)\text{sech}^3(k(y-b))\text{sech}^3(k(y+b)) \\ &\quad + k^2\text{sech}^3(ky)(2\text{sech}(k(y-b)) + (\cosh(2k(y+b)) - \cosh(2bk) + \cosh(2ky) + 3) \\ &\quad \left. \times \text{sech}^3(k(y+b)) - 2\sinh^2(bk)\text{sech}^3(k(y-b))) + 2k^2\text{sech}^4(ky) \right]. \quad (23) \end{aligned}$$

For AdS case ($\Lambda_4 < 0$), we change $\Lambda_4 \rightarrow -\Lambda_4$, the solution of dS₄ brane is transformed into that of AdS₄ brane. This result is interesting, since it simplifies the calculation significantly.

So far, we have obtained the background solution of the three cases of thick branes. In more detail, the potential $U(y)$ is the same; however, $V(y)$ and $\lambda(y)$ take different values for they are related to the parameter Λ_4 . For the sake of clarity, by performing the rescaling of the quantities,

$$\tilde{y} = ky, \tilde{b} = kb, \tilde{\Lambda}_4 = \Lambda_4/k^2, \tilde{V}(\tilde{y}) = V(\tilde{y})/k^2, \tilde{U}(\tilde{y}) = U(\tilde{y})/k^2, \tilde{\lambda}(\tilde{y}) = \lambda(\tilde{y}), \quad (24)$$

we can obtain the dimensionless quantities. The profiles of the potential $\tilde{U}(\tilde{y})$ with the increasing of the parameters \tilde{b} are shown in Fig. 2. In Fig. 3, we compare the behaviors of $\tilde{V}(\tilde{y})$ in the three

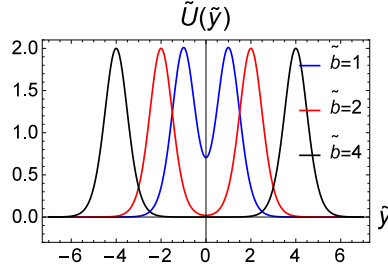


FIG. 2: The potential $\tilde{U}(\tilde{y})$ for the three cases of branes.

cases of thick branes. Figure 3 shows that the potential $\tilde{V}(\tilde{y})$ in AdS₄ brane opens downwards, different from dS₄ brane where the curve opens upwards. When $\Lambda_4 \rightarrow 0$, $\tilde{V}(\tilde{y})$ in dS₄ and AdS₄ branes approach to the values in M₄ brane. The shapes of Lagrange multiplier $\tilde{\lambda}(\tilde{y})$ in terms of $\tilde{y} = ky$ are plotted in Fig. 4. When $\Lambda_4 \rightarrow 0$, $\tilde{\lambda}(\tilde{y})$ in dS₄ and AdS₄ branes also tend to the values in M₄ brane.

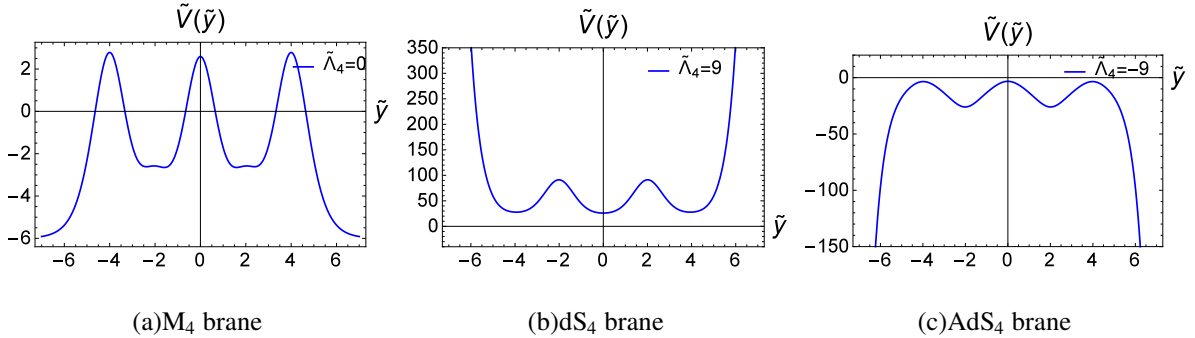


FIG. 3: Comparison of the dimensionless scalar potential $\tilde{V}(\tilde{y})$ in terms of \tilde{y} . The parameter \tilde{b} is set as $\tilde{b} = 4$.

III. LINEAR TENSOR PERTURBATION

In the case of the tensor perturbation, we suppose that the space-time undergoes a small perturbation $\delta g_{MN}^{(1)}$ on a fixed background g_{MN}

$$\tilde{g}_{MN} = g_{MN} + \delta g_{MN}^{(1)}, \quad (25)$$

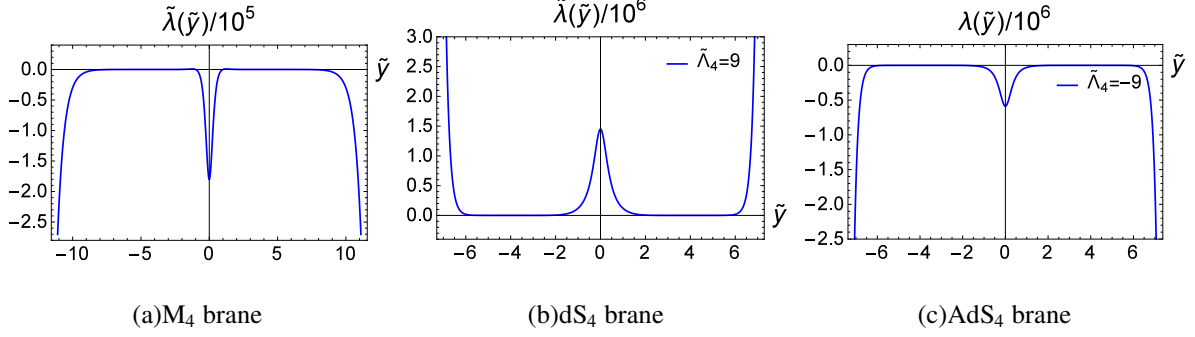


FIG. 4: Comparison of Lagrange multiplier $\tilde{\lambda}(\tilde{\gamma})$ with the parameter $\tilde{b} = 4$.

where g_{MN} represents the five-dimensional Minkowski, dS, or AdS metric. And the inverse of the perturbed metric will be

$$\tilde{g}^{MN} = g^{MN} + \delta g^{MN(1)} + \dots + \delta g^{MN(n)} + \dots \quad (26)$$

with the first-order perturbed metric as $\delta g^{MN(1)} = -g^{MP} g^{NQ} \delta g_{PQ}^{(1)}$ and the n -order perturbed metric as $\delta g^{MN(n)} = (-1)^n \delta g_{P_1}^{M(1)} \delta g_{P_2}^{N(1)} \dots \delta g_{P_n}^{N(1)}$. For the above metric perturbations, the first order perturbations are expressed as follows:

$$\delta \Gamma_{MN}^{L(1)} = \frac{1}{2} g^{LP} \left(\nabla_M \delta g_{NP}^{(1)} + \nabla_N \delta g_{PM}^{(1)} - \nabla_P \delta g_{MN}^{(1)} \right) \quad (27)$$

$$\delta R_{MKN}^{L(1)} = \nabla_K \delta \Gamma_{MN}^{L(1)} - \nabla_N \delta \Gamma_{MK}^{L(1)} \quad (28)$$

$$\delta R_{MN}^{(1)} = \nabla_K \delta \Gamma_{MN}^{K(1)} - \nabla_N \delta \Gamma_{MK}^{K(1)} \quad (29)$$

where ∇_N denotes the covariant derivative corresponding to the five-dimensional metric g_{MN} . In general, it is complicated to take into account a full set of fluctuations of the metric around the background where gravity is coupled to scalars. Fortunately, there is a sector where the metric fluctuations decouple from the scalars, which is the one associated with the transverse and traceless (TT) part of the metric fluctuation. Based on these relations, we will consider the linear tensor perturbation of flat and bent branes by taking the TT gauge condition.

A. Flat brane

For the tensor perturbation of flat brane, the perturbed metric is given by

$$ds^2 = a^2(y)(\eta_{\mu\nu} + h_{\mu\nu})dx^\mu dx^\nu + dy^2, \quad (30)$$

where $\eta_{\mu\nu}$ describes Minkowski geometry, $h_{\mu\nu}$ represents the tensor perturbation and satisfies TT gauge condition $\eta^{\mu\nu}\partial_\mu h_{\lambda\nu} = 0$ and $\eta^{\mu\nu}h_{\mu\nu} = 0$. The linear perturbations of the Ricci tensor and curvature scalar are obtained as

$$\begin{aligned}\delta R_{\mu\nu}^{(1)} &= \frac{1}{2} \left(\partial_\nu \partial_\sigma h_\mu^\sigma + \partial_\mu \partial_\sigma h_\nu^\sigma - \square^{(4)} h_{\mu\nu} - \partial_\mu \partial_\nu h \right) \\ &\quad - (3a'^2 + aa'') h_{\mu\nu} - 2aa' h'_{\mu\nu} - \frac{1}{2} a^2 h''_{\mu\nu} - \frac{1}{2} aa' \eta_{\mu\nu} h', \\ \delta R_{\mu 5}^{(1)} &= \frac{1}{2} \left(\partial_\sigma h_\mu^\sigma - \partial_\mu h \right)', \quad \delta R_{55}^{(1)} = -\frac{1}{2} \left(2a^{-1} a' h' + h'' \right), \\ \delta R^{(1)} &= \delta \left(g^{MN} R_{MN} \right) = a^{-2} \left(\partial_\mu \partial_\nu h^{\mu\nu} - \square^{(4)} h \right) - 5a^{-1} a' h' - h'',\end{aligned}\tag{31}$$

where $\square^{(4)} = \eta^{\mu\nu} \partial_\mu \partial_\nu$ is the four-dimensional d'Alembert operator, and $h = \eta^{\mu\nu} h_{\mu\nu}$.

Under the TT condition, the perturbation of the $\mu\nu$ components of the Einstein tensor reads

$$\delta G_{\mu\nu}^{(1)} = -\frac{1}{2} \square^{(4)} h_{\mu\nu} + (3a'^2 + 3aa'') h_{\mu\nu} - 2aa' h'_{\mu\nu} - \frac{1}{2} a^2 h''_{\mu\nu},\tag{32}$$

where the four-dimensional d'Alembertian is defined as $\square^{(4)} \equiv \eta_{\mu\nu} \partial_\mu \partial_\nu$. Using Eqs. (18) and (32), the perturbation equation reads

$$-\frac{1}{2} \square^{(4)} h_{\mu\nu} - 2aa' h'_{\mu\nu} - \frac{1}{2} a^2 h''_{\mu\nu} = 0.\tag{33}$$

By imposing a coordinate transformation, $dz = \frac{1}{a(z)} dy$ and a rescaling on $h_{\mu\nu} = a(z)^{-3/2} \tilde{h}_{\mu\nu}$, the perturbation equation (33) can be calculated as:

$$\square^{(4)} \tilde{h}_{\mu\nu} + \partial_z^2 \tilde{h}_{\mu\nu} - \frac{\partial_z^2 a^{\frac{3}{2}}(z)}{a^{\frac{3}{2}}(z)} \tilde{h}_{\mu\nu} = 0.\tag{34}$$

Considering the Kaluza-Klein (KK) decomposition $\tilde{h}_{\mu\nu} = \epsilon_{\mu\nu}(x^\gamma) e^{ip_\lambda x^\lambda} H(z)$ with $p^2 = -m^2$, where the polarization tensor $\epsilon_{\mu\nu}$ satisfies the TT condition $\eta^{\mu\nu} \partial_\mu \epsilon_{\lambda\nu} = 0$ and $\eta^{\mu\nu} \epsilon_{\mu\nu} = 0$, we obtain the Schrödinger-like equation for $H(z)$:

$$\left[-\partial_z^2 + V_{\text{eff}}(z) \right] H(z) = m^2 H(z),\tag{35}$$

where m is the mass of the Kaluza-Klein (KK) mode, and the effective potential $V_{\text{eff}}(z)$ is given by [11]

$$V_{\text{eff}}(z) = \frac{\partial_z^2 a^{\frac{3}{2}}(z)}{a^{\frac{3}{2}}(z)} = \left(\partial_z \ln a^{\frac{3}{2}}(z) \right)^2 + \partial_z \left(\partial_z \ln a^{\frac{3}{2}}(z) \right).\tag{36}$$

This equation can be factorized as

$$-\left[\partial_z + \partial_z \ln a^{\frac{3}{2}}(z) \right] \left[\partial_z - \partial_z \ln a^{\frac{3}{2}}(z) \right] H(z) = m^2 H(z),\tag{37}$$

and this structure ensures that the eigenvalues are non-negative, which means that the brane is stable against the tensor perturbation. Since the potential vanishes for large z , this is the only bound state, namely, the massless zero mode ($m = 0$),

$$H_0(z(y)) \propto a^{\frac{3}{2}}(z(y)) = \left[\text{sech}(k(y-b)) + \text{sech}(ky) + \text{sech}(k(y+b)) \right]^{3/2}. \quad (38)$$

To localize the gravity zero-mode, $H_0(z)$ should obey the normalization condition $\int_{-\infty}^{+\infty} |H_0(z)|^2 dz < \infty$. It can be normalized if

$$\begin{aligned} \int_{-\infty}^{+\infty} |H_0(z)|^2 dz &= \int_{-\infty}^{+\infty} |H_0(z(y))|^2 a(y)^{-1} dy \\ &= \int_{-\infty}^{+\infty} \left[\text{sech}(k(y-b)) + \text{sech}(ky) + \text{sech}(k(y+b)) \right]^2 dy < \infty, \end{aligned} \quad (39)$$

which is finite when $k > 0$; in other words, the normalized zero-mode can be achieved for $k > 0$ such that the observable four-dimensional gravity is recovered on the brane. The behaviors of the dimensionless effective potential and zero-mode in terms of \tilde{y} are shown in Fig. 6. The effective potentials have a well with a negative minimum inside the brane and satisfy $V_{\text{eff}}(\tilde{y} \rightarrow \pm\infty) \rightarrow 0$ when far from the brane. As the parameter \tilde{b} increases, the volcano-like potential gradually changes to a multi-well potential, and at last splits into three-well potential; meanwhile, the wave function of the graviton zero-mode also splits.

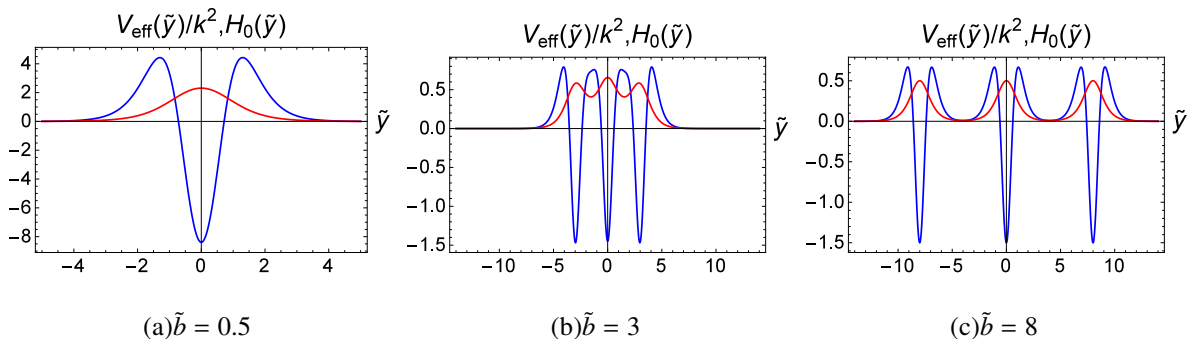


FIG. 5: The influence of \tilde{b} on the dimensionless effective potential $V_{\text{eff}}(\tilde{y})/k^2$ (blue lines) and the zero-mode $H_0(\tilde{y})$ (red lines) of the tensor perturbation for M_4 brane.

B. Bent branes

We now turn to the case of $\Lambda_4 \neq 0$ and consider the following perturbed metric,

$$ds^2 = a^2(y)(\hat{g}_{\mu\nu} + h_{\mu\nu})dx^\mu dx^\nu + dy^2, \quad (40)$$

where the four-dimensional metric is decomposed into a small perturbation $h_{\mu\nu}$ around a curved space-time $a^2(y)\hat{g}_{\mu\nu}$. By imposing a coordinate transformation $dz = \frac{1}{a(z)}dy$, we write the bulk metric in the form

$$ds^2 = a^2(z) \left[(\hat{g}_{\mu\nu} + h_{\mu\nu}) dx^\mu dx^\nu + dz^2 \right]. \quad (41)$$

The interesting investigations of the tensor perturbation have been already appeared in Refs. [56, 57] and in references therein. Then, under the TT gauge condition $h^\mu{}_\mu = \hat{\nabla}^\mu h_{\mu\nu} = 0$, the equation for the perturbation $h_{\mu\nu}$ takes the following form:

$$\left[\partial_z^2 + 3 \left(\partial_z a(z) / a(z) \right) \partial_z + \hat{g}^{\alpha\beta} \hat{\nabla}_\alpha \hat{\nabla}_\beta - \frac{9}{4} \Lambda_4 \right] h_{\mu\nu}(x, z) = 0, \quad (42)$$

where $\hat{\nabla}_\alpha$ denotes the covariant derivative with respect to $\hat{g}_{\mu\nu}$. By performing the KK decomposition $h_{\mu\nu}(x, z) = a(z)^{-3/2} \epsilon_{\mu\nu}(x) H(z)$ with $\epsilon_{\mu\nu}(x)$ satisfying the TT condition, we separate the perturbed equation (42) into the four-dimensional and extra-dimensional part. Here we can get two equations, i.e., $\hat{g}^{\alpha\beta} \hat{\nabla}_\alpha \hat{\nabla}_\beta \epsilon_{\mu\nu}(x) = m^2 \epsilon_{\mu\nu}(x)$ for the four-dimensional part, and the Schrödinger-like equation for the extra-dimensional sector

$$\left[-\partial_z^2 + V_{\text{eff}}(z) \right] H(z) = m^2 H(z). \quad (43)$$

Here m is the mass of the KK mode, and the effective potential is derived as

$$V_{\text{eff}}(z) = -\frac{9}{4} \Lambda_4 + \frac{3}{4} \frac{[\partial_z a(z)]^2}{a(z)^2} + \frac{3}{2} \frac{\partial_z \partial_z a(z)}{a(z)}, \quad (44)$$

for dS_4 geometry. The effective potential can also be transformed in terms of y coordinate,

$$V_{\text{eff}}(z(y)) = -\frac{9}{4} \Lambda_4 + \frac{9}{4} \left[\partial_y a(y) \right]^2 + \frac{3}{2} a(y) \partial_{y,y} a(y), \quad (45)$$

At the boundaries of the brane, the potential $V_{\text{eff}}(z)$ tends to be negative for $\Lambda_4 > 0$. For the term $-\frac{9}{4} \Lambda_4 < 0$, this equation can not be factorized. This result indicates that the tensor perturbation of dS_4 brane would not occur stably. For $\Lambda_4 < 0$, we get AdS_4 geometry, and the potential $V_{\text{eff}}(z)$ tends to be positive at $z \rightarrow \pm\infty$. Eq. (43) can be written as a factorizable equation, $\mathcal{K}\mathcal{K}^\dagger H(z) = m^2 H(z)$ with

$$\mathcal{K} = -\partial_z - \partial_z \ln a^{\frac{3}{2}}(z) + \sqrt{-9\Lambda_4/4}, \quad \mathcal{K}^\dagger = \partial_z - \partial_z \ln a^{\frac{3}{2}}(z) + \sqrt{-9\Lambda_4/4}, \quad (46)$$

which ensures the stability of the tensor perturbation.

IV. MASSIVE RESONANT MODES

For the volcano-like effective potentials, the tensor perturbation has zero-mode and may also have resonant modes. A further investigation of the metastable modes is necessary. Because the integral $z = \int \frac{1}{a(y)} dy$ is difficult, we can not obtain the analytical expressions of the warp factor $a(z)$ and the effective potential $V_{\text{eff}}(z)$. To solve the Schrödinger-like equation (37) for $H(z)$ numerically, we decompose $H(z)$ into an even parity mode and an odd parity mode, which are set to satisfy the following boundary conditions

$$H_{\text{even}}(0) = 1, \quad \partial_z H_{\text{even}}(0) = 0; \quad (47)$$

$$H_{\text{odd}}(0) = 0, \quad \partial_z H_{\text{odd}}(0) = 1. \quad (48)$$

To find the massive resonant states, we use the numerical method given in Refs. [58–61], where a relative probability was proposed:

$$P = \frac{\int_{-z_c}^{z_c} |H_n(z)|^2 dz}{\int_{-z_{\text{max}}}^{z_{\text{max}}} |H_n(z)|^2 dz}. \quad (49)$$

Here $2z_c$ is about the width of the thick brane and z_{max} is set to $z_{\text{max}} = 10z_c$.

A. Flat brane

When the wave functions are either even-parity or odd-parity, the Schrödinger-like equation can be solved numerically. The dimensionless effective potential $V_{\text{eff}}(\tilde{z})/k^2$ is expressed in terms of $\tilde{z} = kz$. Figure 6 shows the influence of \tilde{b} on the effective potential and the resonant modes of gravity. The relative probability P as a function of m^2 is obtained, and only the peak which satisfies $P > 0.1$ represents a resonance mode.

From Fig. 6, we see that, with the increasing of the parameter \tilde{b} the effective potential splits from a single-well into a three-well potential, which indicates there are more resonant KK modes for larger \tilde{b} , and this can be confirmed by Figs. 6(d), 6(e), 6(f). In Fig. 6(d), there are no peaks of the relative probability, which means there does not exist resonant mode. In Fig. 6(e), there is just one peak of the relative probability corresponding to the even-parity or the odd-parity wave function, and its wave functions with mass square $m^2 = 0.3148$ and $m^2 = 1.9633$ are plotted in Fig. 7, which shows that the resonance is indeed quasi-localized on the sub-brane. In Fig. 6(f), we find there are five peaks corresponding to the even-parity or the odd-parity resonant modes which

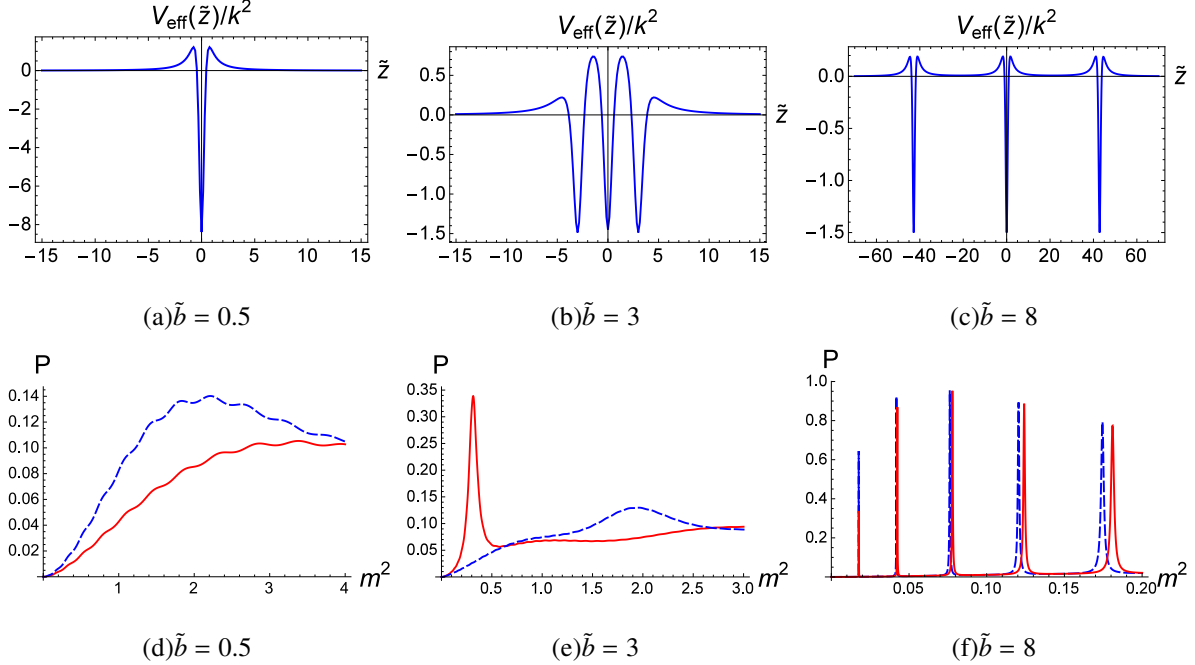


FIG. 6: The influence of the parameter \tilde{b} on the effective potential $V_{\text{eff}}(\tilde{z})/k^2$ and the probabilities P for the odd-parity (blue dashed lines) and even-parity (red lines) massive KK modes.

satisfy $P > 0.1$, and the corresponding wave functions of the first even-parity and odd-parity modes with mass square $m^2 = 0.0177$ and $m^2 = 0.0176$ are plotted in Fig. 7. The numerical results of the mass spectrum, relative probability, full width at half maximum (FWHM) and lifetime of the resonance with $\tilde{b} = 3, 8$ are listed in Tab. I. The resonances having a large lifetime can be quasi-localized on the brane for a long time. Note that the first even and odd resonance modes are not degenerate.

B. Bent branes

Because the tensor perturbation of dS_4 brane would not be stable, we now consider AdS_4 brane, which include two parameters \tilde{b} and $\tilde{\Lambda}_4$. Thus, the resonances are more involved and should be discussed specifically.

The effects of the parameters $\tilde{\Lambda}_4$ on the effective potentials and relative probability are shown in Fig. 8. The effective potentials have a multi-well with a minimum inside the brane and satisfy $\tilde{V}_{\text{eff}}(\tilde{z}) \rightarrow -\frac{2}{3}\tilde{\Lambda}_4$ when $\tilde{z} \rightarrow \pm\infty$. The effective potential does not change its shape but shift up and down with $\tilde{\Lambda}_4$. Therefore, the number of the resonances, the relative probability P , the width of

\tilde{b}	$\tilde{\Lambda}_4$	n	parity	m_n^2	P	Γ	τ
3	0	1	even	0.1988	0.372419	0.00810986	123.307
	0	2	odd	1.8477	0.144147	1.15022	0.8694
8	0	1	odd	0.0176	0.644363	0.00112908	885.681
	0	2	even	0.0177	0.336324	0.00112589	888.186
	0	3	odd	0.0419	0.923572	0.000732362	1365.44
	0	4	even	0.0424	0.850191	0.000727779	1374.04
	0	5	odd	0.0763	0.933456	0.000905549	1104.30
	0	6	even	0.0779	0.94479	0.00089571	1116.43
	0	7	odd	0.1205	0.909459	0.00172875	578.454
	0	8	even	0.1241	0.89555	0.00141991	587.129
	0	9	odd	0.1745	0.792877	0.00215697	278.884
	0	10	even	0.1808	0.755761	0.00358572	404.900

TABLE I: The influence of the parameter \tilde{b} on the mass spectrum m_n , the relative probability P , the width of mass Γ , and the lifetime τ of the KK resonances for the flat brane ($\tilde{\Lambda}_4 = 0$).

mass Γ , and the lifetime τ of the KK resonances do not change with $\tilde{\Lambda}_4$ for a fixed \tilde{b} . Only the mass spectrum changes with $\tilde{\Lambda}_4$. The specific values of masses of the resonances with different values of $\tilde{\Lambda}_4$ (including $\tilde{\Lambda}_4 = 0$) are listed in Tab. II, from which we obtain that all of the masses of the resonances depend linearly on the parameter $\tilde{\Lambda}_4$. For instance, the relations for the masses of the first even-parity and odd-parity modes with $\tilde{b} = 8$ can be expressed as

$$\tilde{m}_{\text{odd}}^2 = 0.0176 - \frac{9}{4}\tilde{\Lambda}_4, \quad (50)$$

$$\tilde{m}_{\text{even}}^2 = 0.0177 - \frac{9}{4}\tilde{\Lambda}_4. \quad (51)$$

We plot the fit functions for masses of the first even-parity and odd-parity modes with different $\tilde{\Lambda}_4$ in Fig. 9. The wave functions for the first even-parity and odd-parity modes with different $\tilde{\Lambda}_4$ are plotted in Fig. 10, which shows that the wave function does not alter with $\tilde{\Lambda}_4$ when \tilde{b} is fixed.

For AdS₄ brane, the potential well also becomes splitting, and the number of resonant modes increases with the parameter \tilde{b} . The influence of the parameter \tilde{b} on the effective potential $V_{\text{eff}}(\tilde{z})/k^2$ and the probabilities P is similar to flat brane, so we do not discuss it repeatedly. Here we list the

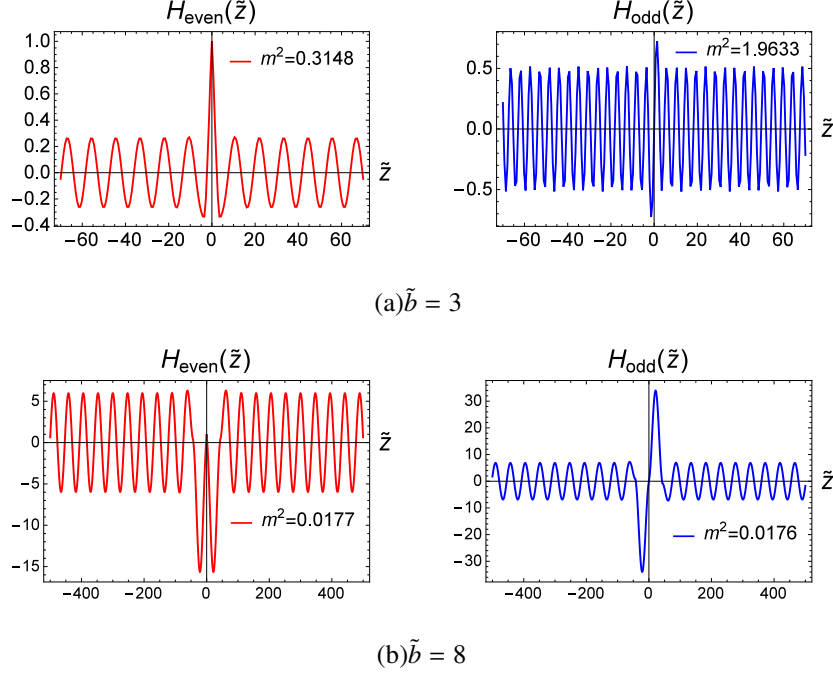


FIG. 7: The wave functions for the first even-parity and odd-parity modes for the flat brane ($\tilde{\Lambda}_4 = 0$) with $\tilde{b} = 3$ and $\tilde{b} = 8$.

numerical results for mass spectrum, the relative probability, the width of mass, and the lifetime of the KK resonances with different \tilde{b} in Tab. III.

V. CONCLUSION

In this paper, we investigate the linear tensor perturbation for M_4 , dS_4 and AdS_4 branes in two-field mimetic gravity. We apply the reconstruction technique to find a set of thick brane solutions in asymptotical AdS_5 space-time, and derive the master equations for linear tensor perturbations under the TT gauge condition. The Schrödinger-like equations for the M_4 and AdS_4 branes are factorized into a supersymmetric form; therefore, the brane systems are stable against the tensor perturbations, while the dS_4 brane is unstable. For the flat and bent branes, the effective potentials of corresponding Schrödinger-like equation behave as volcano-like or modified-volcano-like potentials, which may allow a localized zero-mode responsible for the four-dimensional Newtonian potential and a series of massive resonant modes. The thick branes have two parameters $\tilde{\Lambda}_4$ and \tilde{b} , one for the cosmological constant of the bent brane and the other for the inner structure of the domain wall. We investigate the effect of the two parameters on the thick branes, namely,

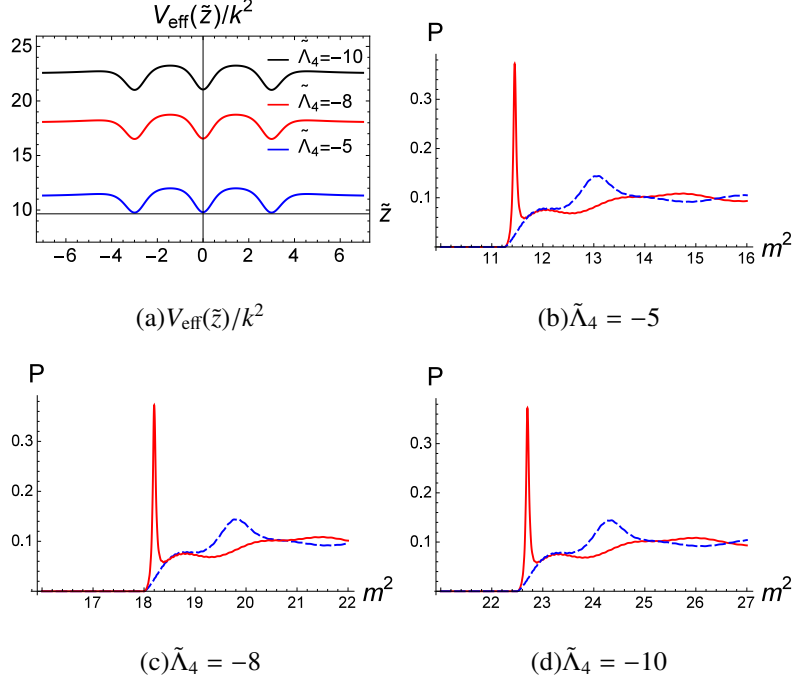


FIG. 8: The influence of the parameter $\tilde{\Lambda}_4$ on the effective potential and the probabilities for both the odd-parity (blue dashed lines) and even-parity (red lines) massive KK modes with a fixed parameter $\tilde{b} = 3$.

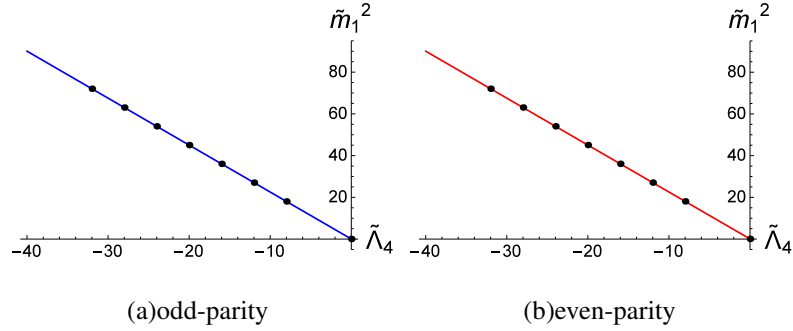


FIG. 9: The influence of $\tilde{\Lambda}_4$ on the masses of the first even-parity and odd-parity modes with $\tilde{b} = 8$. The black dots are numerical results, the solid lines are the fit functions for the first even-parity (red line) and odd-parity (blue line) modes.

- when $\tilde{\Lambda}_4 \rightarrow -\tilde{\Lambda}_4$, the solution of dS₄ changes into that of AdS₄. In the limit $\tilde{\Lambda}_4 \rightarrow 0$, the bent brane solution is reduced to the flat brane solution. The number of the resonances does not change with $\tilde{\Lambda}_4$; however, the masses of resonant KK modes linearly decrease with the parameter $\tilde{\Lambda}_4$ for a fixed \tilde{b} .
- as the parameter \tilde{b} increases, the branes split into sub-branes, and the scalar field $\phi_1(\tilde{y})$

$\tilde{\Lambda}_4 = 0$			$\tilde{\Lambda}_4 = -8$			$\tilde{\Lambda}_4 = -12$		
$\tilde{b} = 3$	$\tilde{b} = 7$	$\tilde{b} = 8$	$\tilde{b} = 3$	$\tilde{b} = 7$	$\tilde{b} = 8$	$\tilde{b} = 3$	$\tilde{b} = 7$	$\tilde{b} = 8$
0.1988	0.047	0.0176	18.1988	18.047	18.0176	27.1988	27.047	27.0176
1.8477	0.0481	0.0177	19.8477	18.0481	18.0177	28.8477	27.0481	27.0177
-	0.1104	0.0419	-	18.1104	18.0419	-	27.1104	27.0419
-	0.1156	0.0424	-	18.1156	18.0424	-	27.1156	27.0424
-	0.199	0.0763	-	18.199	18.0763	-	27.199	27.0763
-	0.2122	0.0779	-	18.2122	18.0779	-	27.2122	27.0779
-	0.3123	0.1205	-	18.3123	18.1205	-	27.3123	27.1205
-	0.3375	0.1241	-	18.3375	18.1241	-	27.3375	27.1241
-	-	0.1745	-	-	18.1745	-	-	27.1745
-	-	0.1808	-	-	18.1808	-	-	27.1808

TABLE II: The influence of the parameter $\tilde{\Lambda}_4$ on the masses m_n^2 of resonances for the KK modes.

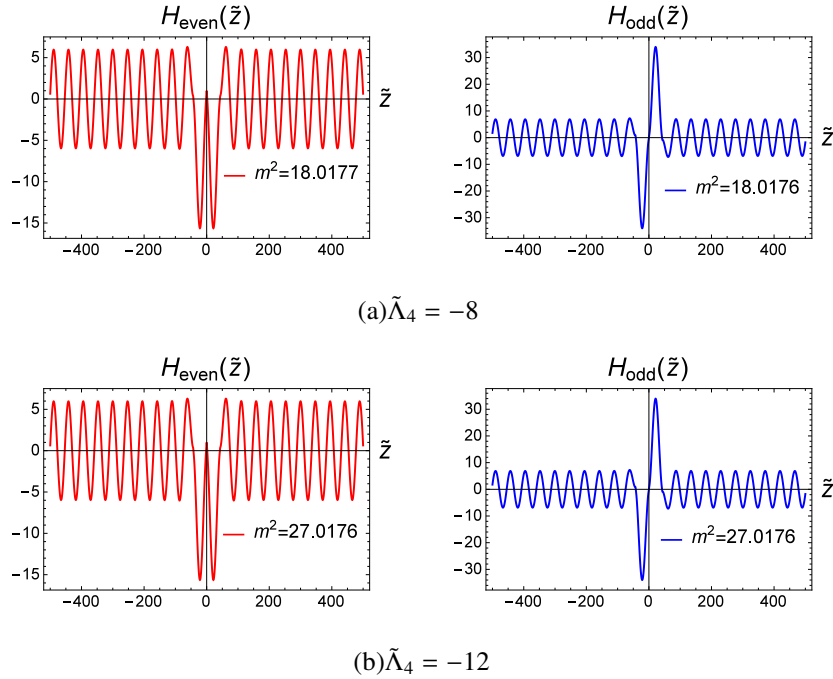


FIG. 10: The wave functions for the first even-parity and first odd-parity modes with $\tilde{b} = 8$.

changes from a single-kink to a double-kink configuration; the effective potentials of the extra-dimensional parts of the tensor perturbations also split into multi-wells; the number of

\tilde{b}	$\tilde{\Lambda}_4$	n	parity	m_n^2	P	Γ	τ
3	-8	1	even	18.1988	0.372419	0.00810986	123.307
		2	odd	19.8477	0.144147	1.15022	0.8694
8	-8	1	odd	18.0176	0.644363	0.00112908	885.681
		2	even	18.0177	0.336324	0.00112589	888.186
		3	odd	18.0419	0.923572	0.000732362	1365.44
		4	even	18.0424	0.850191	0.000727779	1374.04
		5	odd	18.0763	0.933456	0.000905549	1104.30
		6	even	18.0779	0.94479	0.00089571	1116.43
		7	odd	18.1205	0.909459	0.00172875	578.454
		8	even	18.1241	0.89555	0.00141991	587.129
		9	odd	18.1745	0.792877	0.00215697	278.884
		10	even	18.1808	0.755761	0.00358572	404.900

TABLE III: The influence of the parameter \tilde{b} on the mass spectrum m_n^2 , the relative probability P , the width of mass Γ , and the lifetime τ of the KK resonances for AdS₄ brane ($\tilde{\Lambda}_4 = -8$).

gravitational resonance modes increases.

Finally, we would like to point out that the tensor perturbation of the two-field mimetic gravity model is the same as that of the original single-field mimetic theory [48] and GR. Nevertheless, the two mimetic scalar fields can generate different thick branes, leading to new types of effective potential and graviton resonant modes.

Acknowledgements

We sincerely thank Prof. Yu-Xiao Liu for helpful discussions. This work was supported by the National Natural Science Foundation of China (Grants No. 11705070) and the Fundamental Research Fund for Physics of Lanzhou University (No. Lzujbky-2019-ct06). Yi Zhong was supported

by the Fundamental Research Funds for the Central Universities (Grants No. 531118010195).

- [1] N. Arkani-Hamed, S. Dimopoulos and G. R. Dvali, Phys. Lett. B **429** (1998), 263-272 [arXiv:hep-ph/9803315 [hep-ph]].
- [2] I. Antoniadis, N. Arkani-Hamed, S. Dimopoulos and G. R. Dvali, Phys. Lett. B **436** (1998), 257-263 [arXiv:hep-ph/9804398 [hep-ph]].
- [3] L. Randall and R. Sundrum, Phys. Rev. Lett. **83** (1999), 3370-3373 [arXiv:hep-ph/9905221 [hep-ph]].
- [4] L. Randall and R. Sundrum, Phys. Rev. Lett. **83** (1999), 4690-4693 [arXiv:hep-th/9906064 [hep-th]].
- [5] M. Gremm, Phys. Lett. B **478** (2000), 434-438 [arXiv:hep-th/9912060 [hep-th]].
- [6] O. DeWolfe, D. Z. Freedman, S. S. Gubser and A. Karch, Phys. Rev. D **62** (2000), 046008 [arXiv:hep-th/9909134 [hep-th]].
- [7] S. Kobayashi, K. Koyama and J. Soda, Phys. Rev. D **65** (2002), 064014 [arXiv:hep-th/0107025 [hep-th]].
- [8] D. Bazeia, L. Losano and C. Wotzasek, Phys. Rev. D **66** (2002), 105025 [arXiv:hep-th/0206031 [hep-th]].
- [9] A. Wang, Phys. Rev. D **66** (2002), 024024 [arXiv:hep-th/0201051 [hep-th]].
- [10] D. Bazeia and A. R. Gomes, JHEP **05** (2004), 012 [arXiv:hep-th/0403141 [hep-th]].
- [11] V. I. Afonso, D. Bazeia and L. Losano, Phys. Lett. B **634** (2006), 526-530 [arXiv:hep-th/0601069 [hep-th]].
- [12] D. Bazeia, F. A. Brito and L. Losano, JHEP **11** (2006), 064 [arXiv:hep-th/0610233 [hep-th]].
- [13] C. Bogdanos, A. Dimitriadis and K. Tamvakis, Phys. Rev. D **74** (2006), 045003 [arXiv:hep-th/0604182 [hep-th]].
- [14] V. Dzhunushaliev, V. Folomeev and M. Minamitsuji, Rept. Prog. Phys. **73** (2010), 066901 [arXiv:0904.1775 [gr-qc]].
- [15] Y. X. Liu, Y. Zhong and K. Yang, EPL **90** (2010) no.5, 51001 [arXiv:0907.1952 [hep-th]].
- [16] N. Barbosa-Cendejas and A. Herrera-Aguilar, JHEP **10** (2005), 101 [arXiv:hep-th/0511050 [hep-th]].
- [17] A. Herrera-Aguilar, D. Malagon-Morejon and R. R. Mora-Luna, JHEP **11** (2010), 015 [arXiv:1009.1684 [hep-th]].
- [18] Y. Zhong and Y. X. Liu, Eur. Phys. J. C **76** (2016) no.6, 321 [arXiv:1507.00630 [hep-th]].
- [19] V. A. Rubakov and M. E. Shaposhnikov, Phys. Lett. B **125** (1983), 139.

- [20] A. H. Chamseddine and V. Mukhanov, *JHEP* **11** (2013), 135 [arXiv:1308.5410 [astro-ph.CO]].
- [21] A. H. Chamseddine, V. Mukhanov and A. Vikman, *JCAP* **06** (2014), 017 [arXiv:1403.3961 [astro-ph.CO]].
- [22] E. A. Lim, I. Sawicki and A. Vikman, *JCAP* **05** (2010), 012 [arXiv:1003.5751 [astro-ph.CO]].
- [23] E. Babichev and S. Ramazanov, *Phys. Rev. D* **95** (2017) no.2, 024025 [arXiv:1609.08580 [gr-qc]].
- [24] N. Sadeghnezhad and K. Nozari, *Phys. Lett. B* **769** (2017), 134-140 [arXiv:1703.06269 [gr-qc]].
- [25] A. Casalino, M. Rinaldi, L. Sebastiani and S. Vagnozzi, *Phys. Dark Univ.* **22** (2018), 108 [arXiv:1803.02620 [gr-qc]].
- [26] A. Ganz, N. Bartolo, P. Karmakar and S. Matarrese, *JCAP* **01** (2019), 056 [arXiv:1809.03496 [gr-qc]].
- [27] Y. Zheng, L. Shen, Y. Mou and M. Li, *JCAP* **08** (2017), 040 [arXiv:1704.06834 [gr-qc]].
- [28] R. Myrzakulov, L. Sebastiani, S. Vagnozzi and S. Zerbini, *Class. Quant. Grav.* **33** (2016) no.12, 125005 [arXiv:1510.02284 [gr-qc]].
- [29] S. Vagnozzi, *Class. Quant. Grav.* **34** (2017) no.18, 185006 [arXiv:1708.00603 [gr-qc]].
- [30] A. Casalino, M. Rinaldi, L. Sebastiani and S. Vagnozzi, *Class. Quant. Grav.* **36** (2019) no.1, 017001 [arXiv:1811.06830 [gr-qc]].
- [31] O. Malaeb, *Phys. Rev. D* **91** (2015) no.10, 103526 [arXiv:1404.4195 [gr-qc]].
- [32] M. Chaichian, J. Kluson, M. Oksanen and A. Tureanu, *JHEP* **12** (2014), 102 [arXiv:1404.4008 [hep-th]].
- [33] K. Takahashi and T. Kobayashi, *JCAP* **11** (2017), 038 [arXiv:1708.02951 [gr-qc]].
- [34] Y. Zheng, Y. L. Zheng [arXiv:1810.03826 [gr-qc]].
- [35] L. Y. Shen, Y. L. Zheng and M. Z Li, *JCAP* **12** (2019), 026 [arXiv:1909.01248 [gr-qc]].
- [36] S. Nojiri and S. D. Odintsov, *Mod. Phys. Lett. A* **29** (2014) no.40, 1450211 [arXiv:1408.3561 [hep-th]].
- [37] S. Nojiri, S. D. Odintsov and V. K. Oikonomou, *Phys. Rev. D* **94** (2016) no.10, 104050 [arXiv:1608.07806 [gr-qc]].
- [38] S. Nojiri, S. D. Odintsov and V. K. Oikonomou, *Class. Quant. Grav.* **33** (2016) no.12, 125017 [arXiv:1601.07057 [gr-qc]].
- [39] S. D. Odintsov and V. K. Oikonomou, *Phys. Rev. D* **93** (2016) no.2, 023517 [arXiv:1511.04559 [gr-qc]].
- [40] S. D. Odintsov and V. K. Oikonomou, *Annals Phys.* **363** (2015) 503 [arXiv:1508.07488 [gr-qc]].
- [41] A. V. Astashenok, S. D. Odintsov and V. K. Oikonomou, *Class. Quant. Grav.* **32** (2015) no.18, 185007

- [arXiv:1504.04861 [gr-qc]].
- [42] S. Nojiri, S. D. Odintsov and V. K. Oikonomou, *Phys. Lett. B* **775** (2017) 44 [arXiv:1710.07838 [gr-qc]].
- [43] G. Cognola, R. Myrzakulov, L. Sebastiani, S. Vagnozzi and S. Zerbini, *Class. Quant. Grav.* **33** (2016) no.22, 225014 [arXiv:1601.00102 [gr-qc]].
- [44] N. Hosseinkhan and K. Nozari, *Eur. Phys. J. Plus* **133** (2018) no.2, 50
- [45] W. D. Guo, Y. Zhong, K. Yang, T. T. Sui and Y. X. Liu, *Phys. Lett. B* **800** (2020), 135099 [arXiv:1805.05650 [hep-th]].
- [46] J. Chen, W. D. Guo and Y. X. Liu, [arXiv:2011.03927 [gr-qc]].
- [47] S. Davood Sadatian and A. Sepehri, *Mod. Phys. Lett. A* **34** (2019) no.21, 1950162
- [48] Y. Zhong, Y. Zhong, Y. P. Zhang and Y. X. Liu, *Eur. Phys. J. C* **78** (2018) no.1, 45 [arXiv:1711.09413 [hep-th]].
- [49] H. Firouzjahi, M. A. Gorji and S. A. Hosseini Mansoori, *JCAP* **07**, 031 (2017) [arXiv:1703.02923 [hep-th]].
- [50] M. A. Gorji, S. A. Hosseini Mansoori and H. Firouzjahi, *JCAP* **01**, 020 (2018) [arXiv:1709.09988 [astro-ph.CO]].
- [51] H. Firouzjahi, M. A. Gorji, S. A. Hosseini Mansoori, A. Karami and T. Rostami, *JCAP* **11** (2018), 046 [arXiv:1806.11472 [gr-qc]].
- [52] D. Bazeia, L. Losano and J. R. L. Santos, *Phys. Lett. A* **377** (2013), 1615-1620 [arXiv:1304.6904 [hep-th]].
- [53] M. Higuchi and S. Nojiri, *Gen. Rel. Grav.* **46** (2014) no.11, 1822 [arXiv:1402.1346 [hep-th]].
- [54] Y. X. Liu, K. Yang and Y. Zhong, *JHEP* **10** (2010), 069 [arXiv:0911.0269 [hep-th]].
- [55] Y. X. Liu, H. Guo, C. E. Fu and H. T. Li, *Phys. Rev. D* **84** (2011), 044033 [arXiv:1101.4145 [hep-th]].
- [56] S. Kobayashi, K. Koyama and J. Soda, *Phys. Rev. D* **65** (2002), 064014 [arXiv:hep-th/0107025 [hep-th]].
- [57] A. Karch and L. Randall, *JHEP* **05** (2001), 008 [arXiv:hep-th/0011156 [hep-th]].
- [58] Y. X. Liu, C. E. Fu, L. Zhao and Y. S. Duan, *Phys. Rev. D* **80** (2009), 065020 [arXiv:0907.0910 [hep-th]].
- [59] Y. X. Liu, J. Yang, Z. H. Zhao, C. E. Fu and Y. S. Duan, *Phys. Rev. D* **80** (2009), 065019 [arXiv:0904.1785 [hep-th]].
- [60] Y. Z. Du, L. Zhao, Y. Zhong, C. E. Fu and H. Guo, *Phys. Rev. D* **88** (2013), 024009 [arXiv:1301.3204

[hep-th]].

[61] Q. Tan, W. D. Guo, Y. P. Zhang and Y. X. Liu, [arXiv:2008.08440 [gr-qc]].